DOI: 10.1016/j.ejmp.2017.04.005

Dose Painting by means of Monte Carlo Treatment Planning at the voxel level

E. Jiménez-Ortega[1,2], A. Ureba[1,2], A. Vargas[1], J. A. Baeza[1], A. Wals-Zurita[1], F. J. García-Gómez[1], A. R. Barbeiro[1], A. Leal[1,2].

1. Dpto. de Fisiología Médica y Biofísica, Facultad de Medicina, Universidad de Sevilla, Seville, Spain.
2. Instituto de Biomedicina de Sevilla, IBIS, Sevilla, Spain.
3. Hospital Universitario Virgen Macarena, Servicio de Medicina Nuclear, Seville, Spain.
4. Hospital Universitario Virgen Macarena, Servicio de Radioterapia, Seville, Spain.

Abstract

Purpose

To develop a new optimization algorithm to carry out true dose painting by numbers (DPBN) planning based on full Monte Carlo (MC) calculation.

Methods

Four configurations with different clustering of the voxel values from PET data were proposed. An optimization method at the voxel level under Lineal Programming (LP) formulation was used for an inverse planning and implemented in CARMEN, an in-house Monte Carlo treatment planning system.

Results

Beamlet solutions fulfilled the objectives and did not show significant differences between the different configurations. More differences were observed between the segment solutions. The plan for the dose prescription map without clustering was the better solution.

Conclusions

LP optimization at voxel level without dose-volume restrictions can carry out true DPBN planning with the MC accuracy.

Keywords:
Dose painting by numbers, dose painting by contour, linear programming optimization, Monte Carlo dose calculation

Introduction

Nowadays, tumor heterogeneity is one important factor to be considered in radiation therapy. Functional information, as positron emission tomography (PET) or functional magnetic resonance imaging (fMRI), provides us image data associated to tumor progression and potential recurrence after therapy. Moreover, recent studies are based on the hypothesis that boosting volumes with high standard uptake value (SUV) on the pre-treatment ^{18}F-fluoro-deoxyglucose (FDG)-PET scan potentially increases local control while maintaining acceptable toxicity levels [1-4].

The strategy for delivering a non-uniform dose distribution with a prescription based on functional information from medical images is called dose painting (DP) [5, 6]. There are two approaches to carry out the DP strategy: threshold-based dose painting by contours (DPBC) [7] and voxel-based dose painting by numbers (DPBN) [8]. In DPBC, sub-volumes within the tumor are differentiated in the functional images in order to be treated with an escalated dose level. In DPBN, an individual dose prescription is assigned to each voxel within the tumor, varying according to the voxel value in the functional image. These individual doses are usually represented in a dose prescription map.

Tumour sub-volumes can be implemented in commercial treatment planning systems (TPS) to calculate a planning treatment with an escalated dose. Simultaneous integrated boost (SIB) is usually the used technique to achieve this dose. However, as far as we know, planning of DPBN at voxel level is not supported by any commercial TPS [9]. Some DPBN approximations have been made, by introducing sub-volumes as targets [10] or dose maps with prescription to the voxel as objective function [9], but always by using dose-volume based optimization algorithms.

The purpose of this work is to present a new optimization algorithm based on LP to carry out true DPBN planning. This algorithm is able to implement directly constraints to voxels instead of volumes. Furthermore, we propose full Monte Carlo (fMC) calculation in our model as the adequate tool for planning so demanding dose prescription maps as those involved in DPBN.

Material and Methods

Imaging protocol and image analysis

Images were acquired with a Siemens Biograph mCT 64 PET/CT scanner. FDG-PET images were reconstructed with OSEM3D (Ordered Subset Expectation Maximization in three dimensions) algorithm, with 2 iterations and 8 subsets. A post-reconstruction 2 mm Gaussian filter was used for dataset smoothing. A 200 x 200 image-matrix with a pixel size of 4 mm and a slice thickness of 3 mm was obtained. CT-based attenuation correction method was applied.

A case of non-small cell lung cancer was selected to study our optimization approach for DPBN planning. Breathing movements associated to this disease site were not taken into

account in order to achieve solutions only dependent on the prescription dose scheme proposed as input data for our model. The case was selected due to the current consensual use of FDG-PET for the characterization and staging of non–small cell lung carcinoma (NSCLC). Also, the patient presented two spatially separated adenopathies, being a complex scenario to evaluate the behavior of the new optimization algorithm.

DICOM data were imported in CARMEN TPS [11, 12], an in-house fMC treatment planning system controlled through a MATLAB platform. This software was specifically developed to allow previous image analysis to the optimization process. A primary tumor volume was located in the CT images. Co-registered PET/CT images were also evaluated by using the platform in order to determine the extension of the disease. Another adenopathy was then included together with the PET corrected primary tumor in the planning target volume (PTV). In addition, the organs at risk (OARs) were defined. PET and CT data were interpolated to a grid with 256 x 256 pixels per slice, with a 1.9 x 1.9 x 3 mm voxel size.

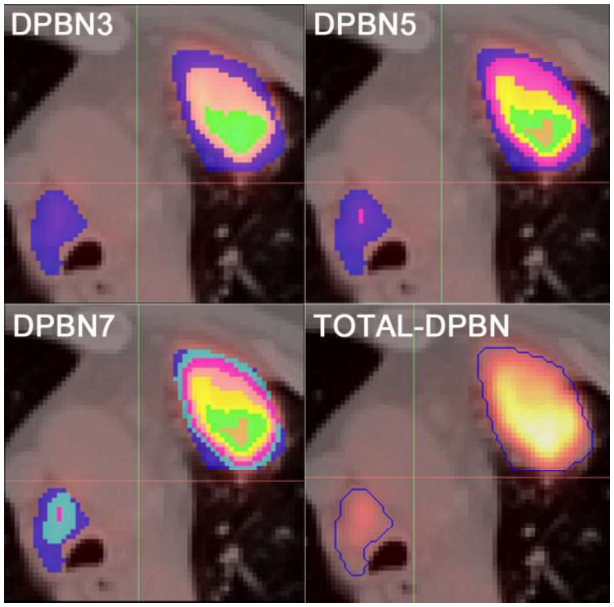

Figure 1. PET/CT fused images at the isocenter slice with the different clustering levels (DPBN3, DPBN5 and DPBN7) and the voxel distribution without clustering (TOTAL-DPBN) generated to establish the dose prescription maps for planning.

In order to make an evaluation consistent with previous published works based on commercial planning systems [10, 13], SUV data from PET images were semi-automatically segmented for clustering. Regarding considerations about essential robust optimization in the case of DPBN related to noise in PET [14, 15], for this study, a specific algorithm based on Affine Propagation (AP) was implemented in CARMEN platform by utilizing a novel intensity affinity metric within the affinity propagation clustering framework [16]. For thresholding purpose, Kernel density estimation (KDE) uses Gaussian kernel but it lacks local adaptation in the PET images histogram. To improve local adaptation, an adaptive KDE is considered by means of the smoothing properties of linear diffusion processes. Also, due to the flexibility of

the AP method, the implemented algorithm generates a novel affinity function that best suited PET image segmentation effectively, where the radiotracer uptake regions is distributed widespread over the region. In this way, this algorithm is able to reflect the diffuse and multifocal nature of the uptake regions, due to uncertainties in object boundaries, low resolution and the inherent noise in PET images. Thus, random errors due to the PET images registration process is reduced becomes our approach in a robust optimization process regarding this kind of uncertainties. Different combinations of parameters were selected to obtain several levels of clustering. The maximum number of different levels distinguished by this algorithm was 7 (DPBN7 in figure 1). In addition, 5 and 3 clustering levels of the SUVs were generated (DPBN5 and DPBN3 in figure 1, respectively). The average SUV of each level was assigned to every voxel of this level. Unlike other works [10], the clusters of voxels were not considered as structures or sub-volumes within the target, since each voxel was treated as an independent entity during the planning process for all configurations. Furthermore, in order to put into value our model, it was also proposed the true option without clustering for planning study exclusively at the voxel level (TOTAL-DPBN in figure 1).

DPBN prescription maps

The dose prescription maps were generated with the same size of the PET/CT calculation grid, assigning zero values to those voxels located out of the PTV. For the voxels within the PTV, it was applied a linear relationship between the prescribed dose and SUV, based on previous work [17]. In this way, the dose value assigned to each voxel is linearly escalated from the minimum to the maximum prescription dose values.

A minimum dose value of 68 Gy, to be delivered in 41 fractions, was assigned, in order to maintain a standard prescribed dose to the conventional target defined only by means of the use of CT images. The maximum prescribed dose was 82 Gy.

Optimization procedure for Monte Carlo planning

Intensity modulated radiation therapy (IMRT) based on an inverse planning was carried out. A novel algorithm based on previous work by our group [11] has been developed, including an optimization method at the voxel level under Lineal Programming (LP) formulation (1), since the usual restriction of dose to volumes makes no sense for DPBN. The optimization consists of minimizing an objective function (min o.f.), in order to fulfill a set of constraints.

$$\min \; o.f. \equiv P_{target}^{max} \sum_{i=1}^{N_{target}} x_i + P_{target}^{min} \sum_{i=1}^{N_{target}} y_i + P_{OAR}^{max} \sum_{i=N_{target}+1}^{N} x_i$$

subject to (1)

$$\sum_{j=1}^{M} \omega_j d_{ij} - x_i \leq D_i^{max} \qquad i = 1, \dots, N_{target}$$

$$\sum_{j=1}^{M} \omega_j d_{ij} + y_i \geq D_i^{min} \qquad i = 1, \dots, N_{target}$$

$$\sum_{j=1}^{M} \omega_j d_{ij} - x_i \leq D_{OAR}^{max} \qquad i = N_{target} + 1, \dots, N$$

$$x_i,\ y_i,\ \omega_j \geq 0 \quad \forall i, j$$

M is the number of beamlets. P_{target}^{max} and P_{target}^{min} represent the penalization factors for the upper and lower dose in each voxel of the target, and P_{OAR}^{max} is the penalization factor for the dose in each voxel of the OARs. These factors are applied to the overdose and underdose vectors, x_i and y_i respectively. d_{ij} and ω_j are matrices with the individual dose coefficients and weights corresponding to each beamlet, respectively. D_i^{max} and D_i^{min} represent the required maximum and minimum dose thresholds for each voxel of the target. D_{OAR}^{max} represents the maximum dose for each voxel of the OARs. N_{target} and N indicate the number of voxels of the target and the total number of voxels implicated in the optimization problem, respectively.

The use of LP makes it possible to distinguish individually each voxel within the involved volumes and allows us to simplify the initial problem by means of a selection of voxels in a specific region. This selection can be also a representative randomized sample of the whole volume with the subsequent reduction on computation time.

On the other hand, faced with the quadratic methods [18], linear programming has clear advantages regarding geometric uncertainties to develop a robust optimization process. With LP it is possible imposing specific constraints to the voxels clearly implied in the uncertainties. In the case of DPBN, these voxels can be those involved in the few differences found in the direct comparison between functional images along the treatment. These considerations for the robustness would increase significantly the number of beamlets and voxels involved in the optimization, but the problem would still be dealt, as it was demonstrated by Chan et al. [19] in their study on robust optimization in LP for IMRT. This feature has not been implemented yet in our algorithm, because more data are needed for a robust formulation.

The planning was calculated to be delivered by a 6 MV photon beam of an Elekta Axesse linac with a multileaf collimator width of 4 mm at isocenter. A phase-space data (PSD), previously simulated with the EGSnrc Monte Carlo user code BEAMnrc [20, 21], was divided into small rectangular regions, in order to generate a grid of finite-sized beamlets for an inverse optimization process. This process is able to find the corresponding weights to produce a fluence or intensity map for each beam. The beamlets dose contribution (BDC) to every voxel of the PTV was calculated using a modified version of the DOSXYZnrc user code [22], named BEAMDOSE [23], implemented in CARMEN platform. The weights of these

BDCs were optimized by using the LP formulation (1). The corresponding fluence maps were subsequently sequenced with an in-house specific sequencer [24] which considers photon interactions with the xMLC based on previous full MC simulations. Besides the obtained segments from the sequencing process, a set of direct apertures based on a 'beam eye view' method was added for all incidences in order to ensure the PTV coverage.

The PSD files corresponding to the segments were obtained with BEAMnrc at the bottom of linac head. Dose contributions of these segments in the voxelized PET/CT were calculated with BEAMDOSE. Finally, the optimal weights representing the final monitor units (MU) for each segment were optimized by the same LP formulation.

All MC simulations were distributed on a cluster of four 12-core 2.19 GHz CPUs AMD Opteron, in a parallel architecture. A grid calculation consisting on 256 × 256 voxels per slice was used, together to a number of beamlets around 1500 for a very high resolution dose calculation able to assess the feasibility of our approach.

Visualization and evaluation of results

The main objective of DPBN process is to be more ambitious by delivering a heterogeneous dose to the target, so the homogeneous coverage of the PTV dose cannot be an adequate criterion to evaluate the quality of the treatment planning [6]. Also, a true DPBN approach should not manage volumes or structures for evaluation of planning, such it is usually done in clinical practice with conventional dose-volume histogram (DVH) and isolines analysis.

Quality index (Q) of the plan has been the evaluation method most used for DPBN strategy [10, 25]. This index is defined as the ratio between the obtained dose with the planning process and the wished dose for each voxel of target. It is graphically represented by a cumulative quality index volume histogram (QVH). The ideal QVH is a step function with Q=1 for all the voxels of the target. $Q_{0.95\text{-}1.05}$ value was evaluated for the treatment plans, defined as the fraction of the voxels of the PTV receiving 95% - 105% of the prescribed dose. In order to evaluate the target and the OARs together (that is, in the same QVH), the dose received by each OAR and the corresponding dose toxicity value was divided by the lowest prescribed dose value, obtaining a representation relative to this dose value. Therefore, OARs dose toxicity values could be also represented in the same histogram. A visualization of spatial distribution of Q values was also developed for analyzing axial slices, in order to evaluate potential overdosage and underdosage zones in target.

Results and discussion

The total planning time spent ranged from 6 to 8 hours. The necessary times spent for each stage in the whole planning process were around the following: 30 minutes for beamlets dose calculation; 30 minutes for beamlets weights optimization; 180 minutes for segments dose calculation and 200 minutes for segments weights optimization. It is necessary to remark that the optimization is a sequential process so it is not suitable for parallelization. For this work, a demanding calculation was considered in order to link the results exclusively to the approach, leaving aside the level of resolution, which could be relaxed for more efficient

process in a clinical application scenario.

Table 1 shows the resulting parameters of the planning process for the four configurations. The $Q_{0.95\text{-}1.05}$ values increased when the dose prescription maps were more heterogeneous, both for beamlets and segment solutions. Higher heterogeneity in dose prescription maps leaded the high gradients become slow dose transitions between the neighboring clusters, simplifying the optimization problem. The needed segments number to achieve the dose distributions was lower for the configurations with lower clustering level, being the monitor units number high for all cases.

Table 1. Characteristics of the plans obtained for the cases with different clustering levels of voxels (DPBN3, DPBN5 AND DPBN7), and the case without any cluster of voxels (TOTAL DPBN).

Study	$Q_{0.95\text{-}1.05}$ (beamlets)	$Q_{0.95\text{-}1.05}$ (segments)	Segments number	MU/fraction
DPBN3	93.3%	86.9%	235	2337
DPBN5	97.7%	91.8%	235	2286
DPBN7	98.1%	95.6%	291	2157
TOTAL-DPBN	97.8%	95.7%	351	2057

Figure 2 shows the QVHs corresponding to the 4 proposed configurations for DPBN approach planned by our model. Theoretical beamlet solutions (dashed lines) and deliverable segment solutions (solid lines) are represented. Beamlet solutions did not show significant differences between the 4 configurations, what indicated a correct behavior of the proposed LP formulation. More differences can be observed for the 4 segment solutions, what was related to the different contribution of beam modifiers to achieve each solution and the associated secondary radiation. The dose to the OARs increased considerably regarding the beamlet solutions due to the scattering, transmission and dose leakage from the MLC. However, these undesirable doses remained under the corresponding toxicity levels for the OARs. For all configurations, the segmentation process led to a group of segments which reproduced efficiently the fluence maps, and therefore, achieving Q values for the target close to 1 in most of voxels, as can be observed in Table 1. Unexpectedly, the larger the proposed number of clusters, the better solution was achieved. Even more, the plan with the dose prescription map without clustering was slightly the better solution.

For all configurations, the conventional target was adequately covered with the standard prescribed dose by means of segments solutions, but a larger volume of body received lower doses, due to a higher secondary radiation than usual. This effect is strongly dependent on the collimation device able to deliver the plan, and it was not observed for all the beamlets solutions. The role of beam modifiers had to be more relevant to achieve so demanding heterogeneous dose distributions. As an example, dose distribution for the TOTAL-DPBN configuration is shown in figure 3 (top).

Figure 3 (bottom) represents the spatial distribution of the Q values for the same case, showing an excellent agreement between the planned dose and the prescribed dose. Only a low number of voxels appeared underdosed, and none of the voxels appeared overdosed.

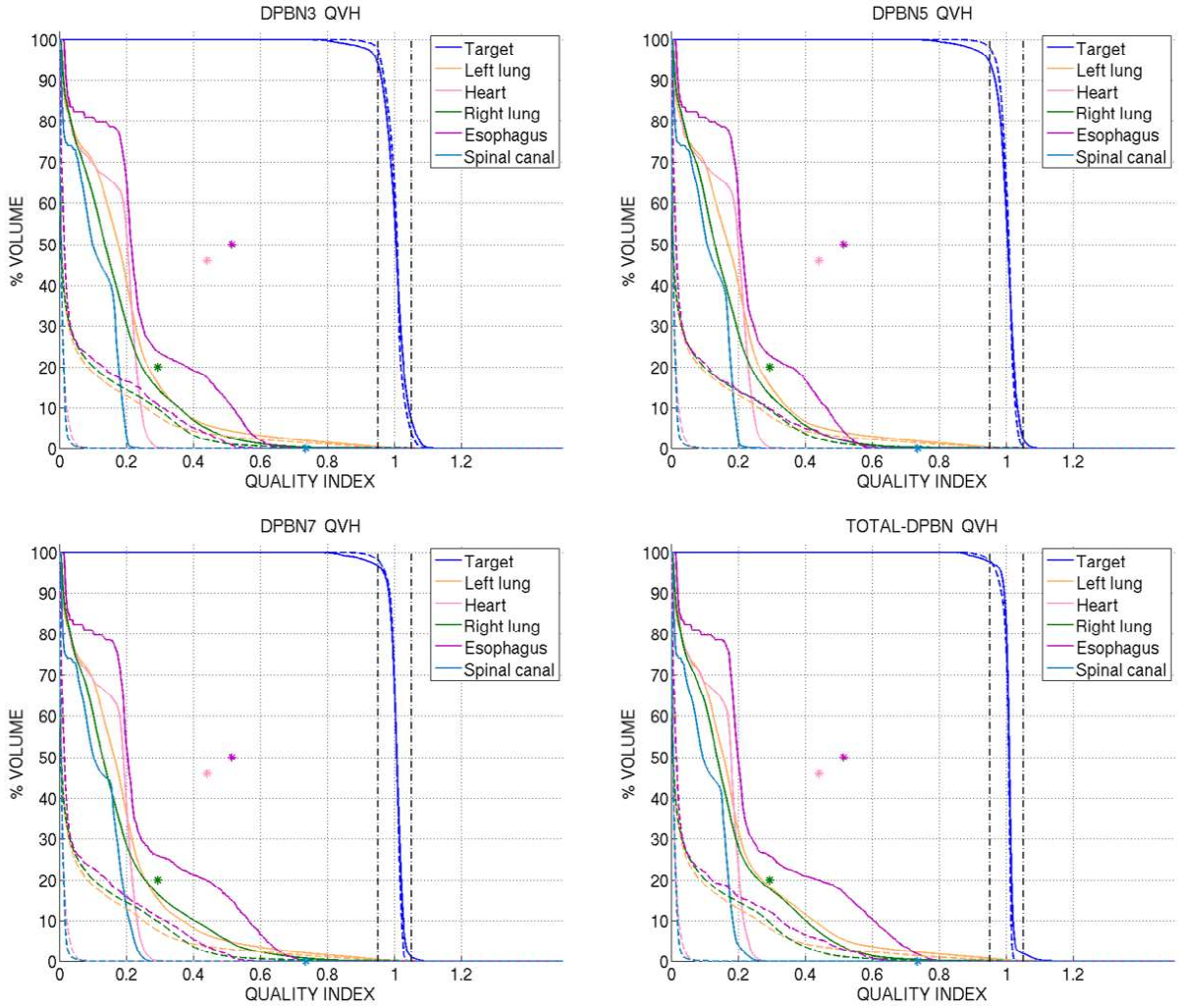

Figure 2. QVH for 3, 5, 7 and none clustering levels, obtained for beamlet solutions (dashed lines) and for segment solutions (solid lines). Points with the same color that the lines corresponding to OARs indicate the usual toxicity level relative to the lower prescription dose. Dash-dot vertical lines represent the values 0.95 and 1.05 of Q.

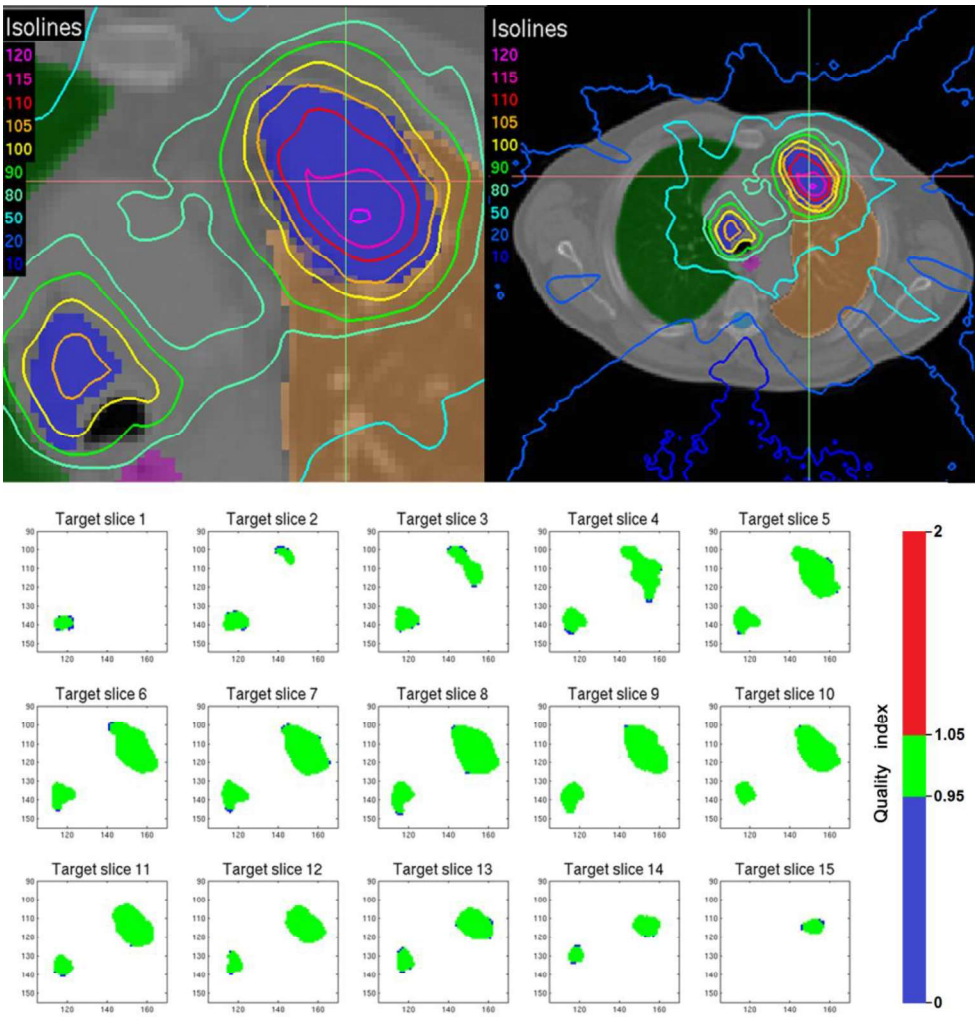

Figure 3. Segments solution for the TOTAL-DPBN configuration. Top, isolines. Bottom, Q index distribution for all axial slices of the target. Green color represents the acceptable quality index values (Q value from 0.95 to 1.05). Red and blue colors represent overdose and underdose regarding the dose prescription map.

Conclusions

A treatment planning process based on full Monte Carlo simulation and under LP optimization can solve the DPBN approach with accuracy and following a robust optimization process. The results showed that DPBN technique works as a guide for the optimization process by setting the necessary gradients for achieving the heterogeneous solution according to the dose prescription map. The final result for delivery is strongly dependent on the used collimation system device. Planning to be delivered by MLC could generate a dose spillage too high to the body. Other models of MLC with lower interleaf transmission could achieve better solutions than obtained in this work. Efforts are being made to obtain segments with a larger area and lower shield, as well as to perform a DPBN planning for VMAT, where the dose spillage could be reduced. Anyway, future works will be focused to extend our model to tomotherapy device, CyberKnife system or hadrontherapy to analyze the degeneration degree from beamlet solution inherent to each delivery system.

References

[1] Lovinfosse P, Janvary ZL, Coucke P, Jodogne S, Bernard C, Hatt M, et al. FDG PET/CT texture analysis for predicting the outcome of lung cancer treated by stereotactic body radiation therapy. European Journal of Nuclear Medicine and Molecular Imaging. 2016;43:1453-60.

[2] Wang JS, Zheng JN, Tang TY, Zhu F, Yao YH, Xu J, et al. A Randomized Pilot Trial Comparing Position Emission Tomography (PET)-Guided Dose Escalation Radiotherapy to Conventional Radiotherapy in Chemoradiotherapy Treatment of Locally Advanced Nasopharyngeal Carcinoma. Plos One. 2015;10.

[3] Yu W, Cai XW, Liu Q, Zhu ZF, Feng W, Zhang Q, et al. Safety of dose escalation by simultaneous integrated boosting radiation dose within the primary tumor guided by (18)FDG-PET/CT for esophageal cancer. Radiotherapy and Oncology. 2015;114:195-200.

[4] Lambin P, van Stiphout R, Starmans MHW, Rios-Velazquez E, Nalbantov G, Aerts H, et al. Predicting outcomes in radiation oncology-multifactorial decision support systems. Nature Reviews Clinical Oncology. 2013;10:27-40.

[5] Ling CC, Humm J, Larson S, Amols H, Fuks Z, Leibel S, et al. Towards multidimensional radiotherapy (MD-CRT): Biological imaging and biological conformality. International Journal of Radiation Oncology Biology Physics. 2000;47:551-60.

[6] Thorwarth D, Geets X, Paiusco M. Physical radiotherapy treatment planning based on functional PET/CT data. Radiotherapy and Oncology. 2010;96:317-24.

[7] Alber M, Paulsen F, Eschmann SM, Machulla HJ. On biologically conformal boost dose optimization. Phys Med Biol. 2003;48:N31-5.

[8] Bentzen SM. Theragnostic imaging for radiation oncology: dose-painting by numbers. Lancet Oncology. 2005;6:112-7.

[9] Arnesen MR, Knudtsen IS, Rekstad BL, Eilertsen K, Dale E, Bruheim K, et al. Dose painting by numbers in a standard treatment planning system using inverted dose prescription maps. Acta Oncol. 2015;54:1607-13.

[10] Korreman SS, Ulrich S, Bowen S, Deveau M, Bentzen SM, Jeraj R. Feasibility of dose painting using volumetric modulated arc optimization and delivery. Acta oncologica (Stockholm, Sweden). 2010;49:964-71.

[11] Ureba A, Salguero FJ, Barbeiro AR, Jimenez-Ortega E, Baeza JA, Miras H, et al. MCTP system model based on linear programming optimization of apertures obtained from sequencing patient image data maps. Medical Physics. 2014;41:216-30.

[12] Baeza JA, Ureba A, Jimenez-Ortega E, Barbeiro AR, Lagares JI, Plaza AL. SU-E-T-157: CARMEN: A MatLab-Based Research Platform for Monte Carlo Treatment Planning (MCTP) and Customized System for Planning Evaluation. Medical Physics. 2015;42:3367-8.

[13] Deveau MA, Bowen SR, Westerly DC, Jeraj R. Feasibility and Sensitivity Study of Helical Tomotherapy for Dose Painting Plans. Acta oncologica (Stockholm, Sweden). 2010;49:991-6.

[14] Differding S, Sterpin E, Janssens G, Hanin FX, Lee JA, Gregoire V. Methodology for adaptive and robust FDG-PET escalated dose painting by numbers in head and neck tumors. Acta oncologica. 2016;55:217-25.

[15] Sterpin E, Differding S, Janssens G, Geets X, Gregoire V, Lee JA. Generation of prescriptions robust against geometric uncertainties in dose painting by numbers. Acta oncologica. 2015;54:253-60.

[16] Foster B, Bagci U, Xu ZY, Dey B, Luna B, Bishai W, et al. Segmentation of PET Images for Computer-Aided Functional Quantification of Tuberculosis in Small Animal Models. Ieee Transactions on Biomedical Engineering. 2014;61:711-24.

[17] Vanderstraeten B, De Gersem W, Duthoy W, De Neve W, Thierens H. Implementation of biologically conformal radiation therapy (BCRT) in an algorithmic segmentation-based inverse

planning approach. Physics in medicine and biology. 2006;51:N277-N86.
[18] Witte M, Shakirin G, Houweling A, Peulen H, van Herk M. Dealing with geometric uncertainties in dose painting by numbers: introducing the DeltaVH. Radiotherapy and oncology : journal of the European Society for Therapeutic Radiology and Oncology. 2011;100:402-6.
[19] Chan TC, Bortfeld T, Tsitsiklis JN. A robust approach to IMRT optimization. Physics in medicine and biology. 2006;51:2567-83.
[20] Kawrakow I, Rogers D. The EGSnrc code system: Monte Carlo simulation of electron and photon transport. 2000.
[21] Rogers D, Walters B, Kawrakow I. BEAMnrc users manual. NRC Report PIRS. 2009;509:12.
[22] Walters B, Kawrakow I, Rogers D. DOSXYZnrc users manual. NRC Report PIRS. 2005;794.
[23] Javier Salguero F, Palma B, Arrans R, Rosello J, Leal A. Modulated electron radiotherapy treatment planning using a photon multileaf collimator for post-mastectomized chest walls. Radiotherapy and Oncology. 2009;93:625-32.
[24] Javier Salguero F, Arrans R, Atriana Palma B, Leal A. Intensity- and energy-modulated electron radiotherapy by means of an xMLC for head and neck shallow tumors. Physics in medicine and biology. 2010;55:1413-27.
[25] Bowen SR, Flynn RT, Bentzen SM, Jeraj R. On the sensitivity of IMRT dose optimization to the mathematical form of a biological imaging-based prescription function. Physics in medicine and biology. 2009;54:1483-501.

Table 1.

Characteristics of the plans obtained for the cases with different clustering levels of voxels (DPBN3, DPBN5 AND DPBN7), and the case without any cluster of voxels (TOTAL DPBN).

Study	$Q_{0.95\text{-}1.05}$ (beamlets)	$Q_{0.95\text{-}1.05}$ (segments)	Segments number	MU/fraction
DPBN3	93.3%	86.9%	235	2337
DPBN5	97.7%	91.8%	235	2286
DPBN7	98.1%	95.6%	291	2157
TOTAL-DPBN	97.8%	95.7%	351	2057

Figure 1

Click here to download high resolution image

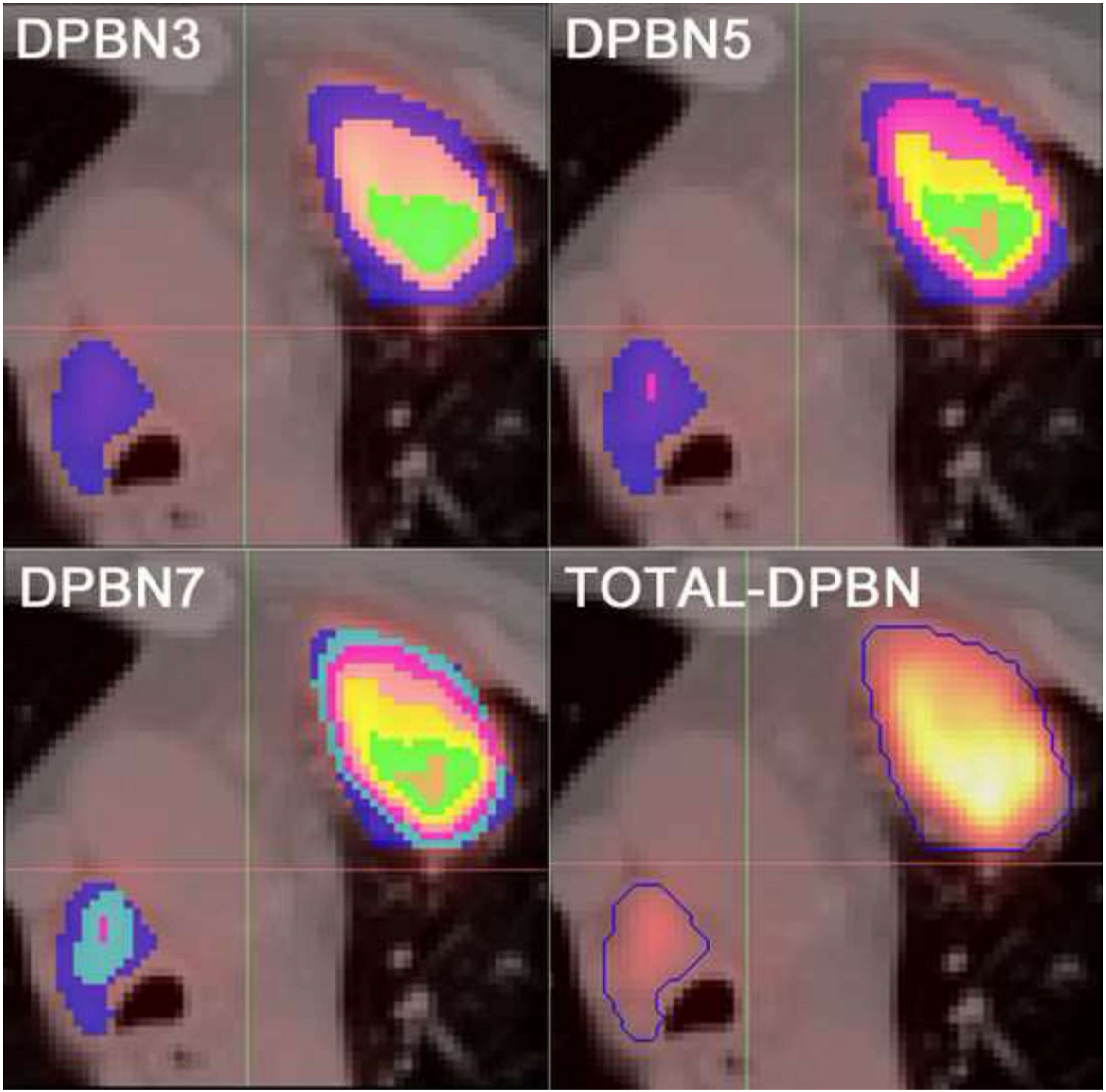

Figure 2

Click here to download high resolution image

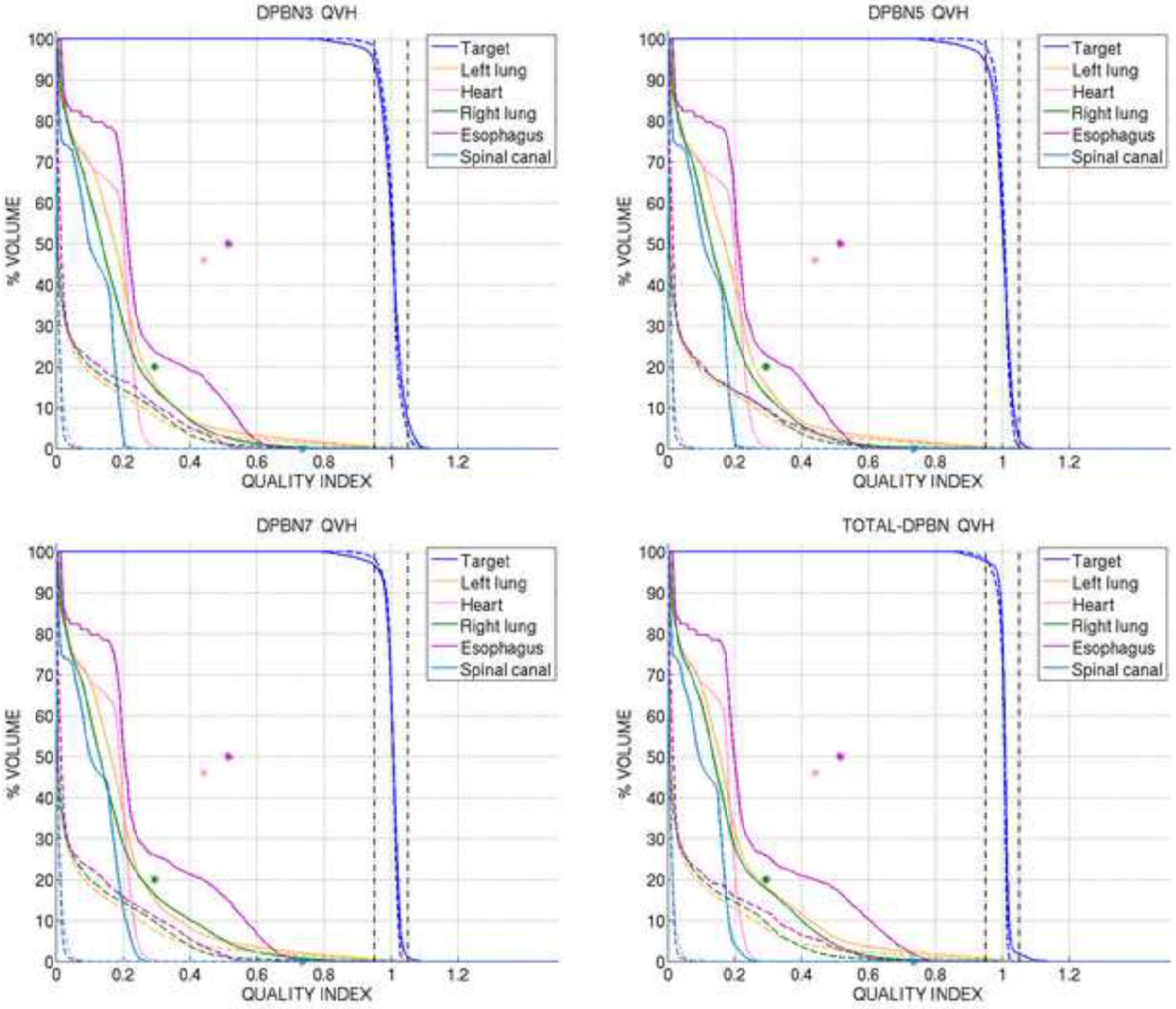

Figure 3

Click here to download high resolution image